U. S. DEPARTMENT OF THE INTERIOR
U. S. GEOLOGICAL SURVEY

ON THE MECHANISM OF THE LARGE HYDRAULIC GRADIENT UNDER YUCCA MOUNTAIN, NEVADA

by

Chris Fridrich
U.S. Geological Survey, Box 25046, MS 913, Denver, CO 80225

Shemin Ge
Department of Geological Sciences, Campus Box 250,
University of Colorado, Boulder, CO 80309

John Sass
U.S. Geological Survey, 2255 Gemini Dr., Flagstaff, AZ 86001

Open-File Report 98-119

March 9, 1998

Abstract

We use coupled fluid- and heat-flow modeling (the TOUGH2 code) to investigate three alternative hydrogeologic models for a steep 300-m water-table decline, known as the large hydraulic gradient (LHG), and a spatially coincident heat-flow low under Yucca Mountain, Nevada: (1) a fault-related **dam** within the volcanic tuff (water-table) aquifer, (2) a **spillway** created by abrupt southward increase in the depth-extent (thickness) and permeability of the tuff aquifer across a fault, and (3) a **drain** formed by a fault that allows the major flow through the tuff aquifer from the north to be captured by the underlying confined carbonate aquifer. All three models provide an adequate simulation of the observed water-table configuration under Yucca Mountain, as well as the shallow thermal regime. None of the models provides an adequate simulation of the deep thermal regime, and the drain model alone can be eliminated on that basis. Our simulations of the dam and spillway models yield strongly contrasting predictions about the pattern of vertical hydraulic gradients in the vicinity of the LHG, suggesting that a well-designed drilling and hydrologic testing program would yield definitive answers about the cause of this feature.

Introduction

Yucca Mountain, which straddles the western boundary of the Nevada Test Site in the southern Great Basin (Figures 1 and 2), has been under intensive study as a potential geological repository site for storing the nation's high-level radioactive waste and spent fuel from nuclear reactors. Because of the exceptionally deep water table under central Yucca Mountain, the potential repository can be constructed in volcanic tuffs 300-400 meters beneath the surface, and yet be 200-400 meters above the current water table. The design concept is to create a "mummy's tomb" in which the waste would be isolated from the surface by the great depth of the repository, and isolated from the saturated-zone groundwater system by the thick unsaturated section between the repository and the water table, as well as by the current low flux of groundwater through the unsaturated zone in the arid climate of southern Nevada.

Whereas the "mummy's tomb" idea is an excellent concept for a radioactive waste repository, it is unclear how well the Yucca Mountain site actually conforms to this concept. For example, the water table abruptly rises at least 300 m immediately to the north of the potential repository area (Figure 2), and is higher than much of the design repository at a distance of 2 km to the north, and perhaps closer. Some paleohydrology studies indicate that the water table was about 100 m higher under central Yucca Mountain in the recent past [Marshall *et al.*, 1993]. Moreover, an extensive perched water zone is present throughout most of the area of the potential repository near the base of the proposed repository horizon [Rousseau *et. al.*, 1996; Hinds *et al.*, 1997], and the presence and behavior of the perched-water system may be genetically linked to the immediately adjacent steep decline in water-table elevation. A National Academy of Sciences panel concluded that "not until the source of the gradient [the ≥300-m water-table decline] is known can the potential hazard that the repository may face due to climate changes and/or tectonic events be evaluated with a high level of confidence" [NRC, 1992].

This paper examines the hydrodynamics of the saturated-zone groundwater regime of Yucca Mountain with emphasis on the mechanism of the 300-m water table decline. Three alternative hypotheses for the cause of the water-table decline are considered. Based on the existing geologic, hydrological, and geophysical data, a two-dimensional cross-sectional conceptual model is constructed and is used to test these hypotheses quantitatively in a series of simulations using TOUGH2, a fully coupled fluid- and heat-flow code [Pruess, 1991].

Hydrogeology of Yucca Mountain

Yucca Mountain is a multiple-fault-block ridge located on the south flank of the southwest Nevada volcanic field, within the Death Valley groundwater system (Figure 1). The configuration of the southeastward-sloping water table under Yucca Mountain is dominated by an abrupt decline of 300 m over a distance of 2 km or less (Figure 2). This northeast-striking zone of large hydraulic gradient (0.15 or more) separates an area of moderate gradient (of about 0.015) to the north from an area of very small gradient (0.0001) to the south. An additional feature of the water-table configuration is a 45-m decline in water-table elevation under western Yucca Mountain, immediately east of Solitario Canyon (Figure 2).

The north-striking 45-m step in the water table coincides spatially with the Solitario Canyon fault. This step evidently results from the damming effect created by offset stratigraphy, specifically the juxtaposition of a confining unit against the water-table aquifer along this major fault [Fridrich *et al.*, 1994]. In contrast, the 300-m water-table decline under northern Yucca Mountain does not correspond to any exposed geologic feature.

Fridrich *et al.* [1994] showed, however, that the 300-m decline, which is commonly known as the large hydraulic gradient, coincides spatially with the northern margin of a trough-like 10-milligal gravity low, and that this gravity low can be explained by the greater thickness of Tertiary volcanic rocks encountered in bore holes drilled within the low in relation to holes drilled to the north and south of it. The gravity anomaly thus reflects a buried depression filled with low-density rocks. The observed stratigraphic thickening into the gravity low is a step change, which indicates that this depression is bounded by growth faults in the deep (>0.5 km depth) Tertiary volcanic section. The large hydraulic gradient is thus interpreted as coinciding with the northern bounding fault of a buried graben as shown in Figure 3 [Fridrich *et al.*, 1994].

The large hydraulic gradient may also coincide, at least roughly, with the north boundary of the deep carbonate aquifer under Yucca Mountain. Yucca Mountain consists of a thick (1.5-3 km) sequence of faulted and weakly tilted Miocene volcanic rocks of the southwest Nevada volcanic field (Figure 1). This Miocene volcanic sequence unconformably overlies a much thicker (>10 km) section of strongly deformed Paleozoic and latest Proterozoic sedimentary rocks, consisting of highly permeable carbonate rocks (limestones and dolomites) and much less permeable clastic rocks (quartzites and argillites). Whereas the water table under Yucca Mountain is located in the upper part of the volcanic section, the major regional groundwater flow is presumed to pass through the

underlying Paleozoic carbonate aquifer [Winograd and Thordarson, 1975]. The deep carbonate aquifer is separated from the volcanic water-table aquifer by the lower tuff confining unit, which consists of the Lithic Ridge Tuff, older tuffs, and underlying unnamed tuffaceous sedimentary rocks (Figure 3).

A single bore hole, UE25-p#1 (Figures 2 and 3), was drilled into rocks underlying the Tertiary volcanic section of Yucca Mountain. This hole encountered the Paleozoic carbonate aquifer, demonstrating its presence under southern Yucca Mountain [Craig and Robison, 1984]. A long-wavelength aeromagnetic anomaly over northernmost Yucca Mountain [Boynton and Vargo, 1963] suggests that the volcanic rocks there are underlain by a strongly magnetic rock unit [Bath and Jahren, 1984]. Bath and Jahren interpreted this magnetic anomaly as an extension of a stronger anomaly to the east, which results from magnetite-bearing hydrothermally altered Paleozoic argillite (originally identified as the Eleana Formation (Argillite)) as shown in Figure 3, but recently reclassified as the Chainman Shale by J. C. Cole, USGS, oral comm., 1997). Bath and Jahren thus inferred that the volcanic rocks under northernmost Yucca Mountain are underlain by argillite instead of carbonate rocks. If their interpretation is correct, then the carbonate aquifer pinches out northward under Yucca Mountain approximately in the position of the large hydraulic gradient [Fridrich *et al.*, 1994].

In the saturated zone under Yucca Mountain, the effective permeable pathways for saturated-zone flow are apparently controlled dominantly by tectonic fracturing, especially the major fault zones that cut through Yucca Mountain [Fridrich *et al.*, 1994]. This is not to say that stratigraphy is unimportant, however, because the development of fracture permeability along tectonic fracture zones is strongly dependent on lithology, especially on changes in welding, crystallization, and other lithologic features that vary through the volcanic section. The units that comprise the principal Tertiary aquifer under Yucca Mountain are the welded tuffs that underlie the water table, especially the Prow Pass, Bullfrog, and Tram Tuffs of the Crater Flat Group (Figure 3). South of the large hydraulic gradient, the densely welded Topopah Spring Tuff is also locally below the water table and is an important aquifer, as discussed below.

In addition to the lateral changes in potentiometric head under Yucca Mountain (the water-table configuration), vertical changes in head have been observed. For example, there is a downward hydraulic gradient under northern Yucca Mountain, based on observations in drill hole USW G-2 [Czarnecki, 1994; Czarnecki *et al.*, 1995]. Thermal observations suggest that this downward gradient extends to a depth of at least 1.3 km [Sass *et al.*, 1988; Czarnecki *et al.*, 1995]. An upward hydraulic gradient has been observed under southern Yucca Mountain in drill hole UE25-p#1; specifically, the head in the carbonate aquifer is about 20 m higher than that in the overlying tuff aquifer in this well [Craig and Robison, 1984]. This southward transition from a downward gradient to an upward gradient across Yucca Mountain is located approximately in the position of the large hydraulic gradient, and is probably just part of the regional pattern as one moves away from the major recharge areas toward the major discharge areas of the hydrologic system.

Thermal Structure under Yucca Mountain

The Great Basin of the western United States is characterized by diverse and complex thermal and hydrologic regimes. The average heat flow is high (100 mWm^{-2}) but there are large regions of both very high and anomalously low heat flow. One such region is the "Eureka Low," which occupies about 35,000 km^2 of a terrain in southeast Nevada (Figure 2, inset map) in which the dominant aquifer consists of Paleozoic limestones and dolomites [Sass *et al.*, 1995]. Conductive heat flows within the Eureka Low are mostly low (<60 mWm^{-2}). There are, however, large areas of high advective flux (e.g., Railroad Valley; Hot Creek Valley] within its boundaries, indicating that the average ambient heat flow for this terrain is similar to that of the rest of the Great Basin, and that the deviations from the average heat flow are the result of redistribution of heat by groundwater flow. The Eureka Low has been interpreted as a relatively shallow (3-4 km) hydrologic feature from both thermal and hydrologic observations [Sass et al.,1971; Winograd and Thordarson, 1975; Lachenbruch and Sass, 1977].

Yucca Mountain is located on the southern margin of the Eureka Low and exhibits considerable thermal variability on the scale of kilometers (Figure 2). In particular, the candidate repository site is within a local heat-flow low that extends from the vicinity of the large hydraulic gradient southward for about 10 km. The heat flows shown here (Figure 2) are from the unsaturated zone, but they are consistent with independent determinations in the saturated zone of drill holes that extend a significant distance below the water table and exhibit conductive thermal profiles [Sass *et al.*, 1988].

Because the apparent width of the local heat-flow low at Yucca Mountain is only about 5 kilometers (Figure 2), we can assume that it originates at comparable or shallower depths. The major cause of low heat flow at Yucca Mountain relative to most of the Great Basin probably is related to processes operating within the carbonate aquifer, because these rocks provide the conduit for the interbasin flow responsible for the larger Eureka Low [Sass *et al.*, 1995]; moreover, the very low temperature for the depth, at the bottom of well UE-25p#1 (54 degrees C at 1800 m), indicates that the thermal anomaly extends into the carbonate aquifer under Yucca Mountain, at least locally.

Shallower processes, however, also play a role in creating the total heat flow anomaly at Yucca Mountain. For example, some unknown rate of groundwater flow presumably occurs southward through the water-table aquifer across the large hydraulic gradient, and the downward component of that flow contributes to the heat-flow anomaly. Evaporative cooling and downward percolation in the unsaturated zone may also contribute; however, existing data indicate that the unsaturated-zone contribution to the heat-flow anomaly is negligible [Sass *et al.*, 1995].

Conceptual Models for the Large Hydraulic Gradient

Whereas the inferred buried graben and northward pinchout of the deep carbonate aquifer under Yucca Mountain discussed above are interpretations, the data that these interpretations are based on are ground truth. For example, even if the buried graben interpretation is wrong in some of its specifics, there must be a large geologic feature of

some kind under the large hydraulic gradient based on the objective data, namely the gravity anomaly and the observed step changes in stratigraphic thicknesses across the boundaries of this anomaly. The most important question about the concealed geologic features that coincide spatially with the large hydraulic gradient is not what their precise geologic character is, but rather what their hydrologic effect is. The geologic interpretations discussed above do not lead to a unique conclusion about the hydrologic cause of the large hydraulic gradient; they do, however, provide a basis upon which to develop alternative conceptual models of the physical mechanism of this hydrologic feature.

Downwelling from the tuff (water-table) aquifer into the deep carbonate aquifer, near the postulated northern limit of the carbonate aquifer, could by itself result in a southward decline in the water table under Yucca Mountain. However, because of the presence of the lower tuff confining unit between the two major aquifers, the zone of downwelling would be spread out laterally across several kilometers unless some additional feature provided a transmissive pathway through the lower tuff confining unit to localize the downwelling into the observed narrow zone of water-table decline. The inferred buried fault that coincides with the large hydraulic gradient could provide the pathway and, if so, this fault is acting as a drain allowing flow in the tuff aquifer, derived from recharge areas to the north, to be largely captured by the deep carbonate aquifer (Figure 4a). We call this the drain model.

Alternatively, the carbonate aquifer may not be involved and the buried fault may, by itself, create the large hydraulic gradient within the volcanic section. There are two major ways that this could work. First, the buried fault may form a barrier to flow in the volcanic section. This is the dam model (Figure 4c).

A more complex, but geologically reasonable model is that the buried fault may act as a spillway. The major tuff aquifer under southern Yucca Mountain is the Crater Flat Group of tuffs. This volcanic group thins strongly and abruptly northward across the large hydraulic gradient. The abrupt thinning results in a reduced degree of welding of the tuff units on the upthrown (northern) side and, consequently, in greater susceptibility to permeability-reducing hydrothermal alteration. The upthrown side is also closer to the Miocene heat source for the hydrothermal alteration, the caldera complex at the north end of Yucca Mountain, and the rocks under northern Yucca Mountain are, in fact, significantly more altered than those to the south [Bish, 1989]. If large-scale permeability is strongly reduced northward across this buried fault, then the buried fault under the large hydraulic gradient may be the effective northern boundary of the tuff aquifer under Yucca Mountain. The small flow of groundwater that comes through the tuffs to the north probably would flow dominantly through the less altered upper part of the tuff section, and then suddenly descend, in spillway fashion, into the tuff aquifer where it abruptly begins on the downthrown side of the fault (Figure 4b).

The drain, dam, and spillway models differ mainly in the physical arrangement of the permeability structure and of the resultant flow pathways (Figure 4). In the case of the dam (Figure 4c), permeability and thus flow pathways extend to depth within the tuff section on both sides of the dam, and the fault-dam resists the flow, resulting in a higher water-table elevation on the upgradient side. In the case of the spillway (Figure 4b), the

water table abruptly drops because the effective base of the hydrologic system, and thus of possible flow pathways, abruptly drop within the volcanic section. The drain model (Figure 4a) differs from the spillway model in that the dominant flow is descending into the deep carbonate aquifer, rather than just descending within the volcanic section.

The dam, drain, and spillway models are simple end-member conceptions of the physical mechanism of the large hydraulic gradient under Yucca Mountain that we believe embrace the major range of possible mechanisms for the large hydraulic gradient. For example, the physical arrangements of the permeability structure and of the flow pathways in the spillway model provide a reasonable representation of a model proposed by Czarnecki [1994] and Czarnecki *et al.* [1995] that the large hydraulic gradient is created by the abrupt lateral termination of a perched water table that is 300 m higher than the true water table.

Summary of Past Modeling Efforts

Quantitative assessment of the groundwater flow system in the whole Death Valley basin, of which Yucca Mountain is a very small part (Figure 1), has been conducted previously by several researchers, including Waddell [1982] and Sinton [1989]. The emphasis of these models is on recharge and discharge patterns at a regional scale. The large hydraulic gradient of Yucca Mountain, however, is on a scale of several kilometers and therefore cannot be adequately examined by these regional models.

At a slightly more focused scale, Czarnecki and Waddell [1984] simulated groundwater flow in the hydrologic subbasin in which Yucca Mountain lies using a two-dimensional (plan-view) finite-element model. They used a parameter-estimation technique to calibrate their model with observed hydraulic heads. Their estimated parameters include rock transmissivities and recharge and discharge fluxes at the boundaries of their computational domain. The two-dimensional areal model is restricted to horizontal flow and therefore cannot be applied to areas where vertical flow components are present. By assigning a low-permeability zone in the large hydraulic gradient area, they reproduced this feature as resulting from a dam.

In the same area of the Czarnecki and Waddell model, Haws [1990] performed two-dimensional finite-element modeling of a vertical cross section and concluded that a shallow low-permeability zone in the area of the large hydraulic gradient can produce the observed potentiometric pattern. To examine the effects of infiltration and permeability structure of water-table configuration, Jasek [1991] used a similar technique of inserting a low-permeability zone beneath the large hydraulic gradient to simulate the 300-m water table decline.

In a broad context, all of these previous modeling efforts thus assumed a dam model to explain the large hydraulic gradient.

Design of the Present Modeling Effort

Numerical modeling in this study was undertaken to test alternative hypotheses for the cause of the large hydraulic gradient under Yucca Mountain. Our approach can be

summarized in five points:

(1) We wanted to incorporate as many of the geologic constraints on the Yucca Mountain hydrologic system as possible, while allowing flexibility in associating different hydrologic processes with key geologic features, especially the postulated buried fault under the large hydraulic gradient.

(2) To achieve our goal, the uncertainties associated with the poorly constrained boundary conditions could not be avoided; those uncertainties must, therefore, be taken into account in the analysis of model results. Previous modeling efforts have extended over areas much larger than Yucca Mountain in order to overcome the problem of poorly constrained boundary conditions in the immediate vicinity of the potential repository area. However, exploring the physical processes requires modeling that is focussed on the area of the feature of interest, in this case the large hydraulic gradient.

(3) We were less concerned with achieving an exact calibration in our simulations than with developing an understanding of the physical processes that govern the system. In addition, we did not attempt to match features that we thought might just be local anomalies.

(4) We decided that including the thermal regime in our modeling was critical because it has been shown that the groundwater flow field under Yucca Mountain couples with heat transfer [Sass *et al.*, 1995]. Hence, we used TOUGH2, a code that solves the fluid mass-balance equation and heat conduction-convection equation simultaneously using the integrated finite-difference method. The basic physics behind fluid and heat coupling is that fluid flow redistributes the heat while the temperature gradient modifies the fluid density and viscosity, and consequently the hydraulic conductivity and flow pattern.

(5) The model cross section used was taken from Fridrich *et al.* [1994] and extends in a north-northwest to south-southeast direction across the large hydraulic gradient (Figures 2 and 3). Four wells along this cross section were drilled deep enough to extend through the tuff aquifer into the lower tuff confining unit and have measured thermal profiles: USW G-2, USW G-1, UE25-b#1, and UE25-p#1. With this geologic section as a basis, a mesh was generated with 33 rows and 54 columns over a cross-sectional area that is 3 km deep and 10 km long.

One possible shortcoming associated with the selection of this particular cross section (Figure 3) is that the Topopah Springs Tuff is everywhere above the water table on this section, whereas it locally lies below the water table east and west of this section southward of the large hydraulic gradient (Fridrich *et al.*, 1994). Whereas the Crater Flat Tuffs are fully saturated under all but a very small area under Yucca Mountain, and are therefore considered the major Tertiary aquifer, the Topopah Springs Tuff is only locally saturated, but is significantly more permeable than the Crater Flat Tuffs. A potentially important geologic element that may affect the permeability structure of Yucca Mountain is thus absent in our model. Given the complex three-dimensional character of the structure of Yucca Mountain, there is no single cross section that can totally represent the permeability structure. We address this problem below in interpreting our simulation results.

Hydrostratigraphy

Using the hydrologic features of different lithologic units as a basis, we adopt five major hydrostratigraphic units, as suggested by previous researchers [Winograd and Thordarson, 1975; Fridrich *et al.*, 1994; Waddell *et al.*, 1984]. These include the major tuff aquifer, namely the Crater Flat Group (the Prow Pass, Bullfrog, and Tram Tuffs), and the lower tuff confining unit, which consists of the Tertiary section underlying the Tram Tuff, as discussed above. The Crater Flat aquifer is overlain by the Calico Hills confining unit and by the Tiva Canyon/Topopah Spring aquifer. This uppermost aquifer is almost entirely unsaturated in the area of our cross section (Figure 3). The lower tuff confining unit is underlain by the Paleozoic carbonate aquifer.

In general, the development of fracture permeability in the Tertiary hydrologic units increases with the intensity of welding in the tuffs. In contrast, alteration decreases permeability, especially for the nonwelded tuffs. Some lavas that are locally present under the Tram Tuff under northern Yucca Mountain (Figure 3) are little fractured and are included here as part of the lower tuff confining unit. In general, the carbonate aquifer is highly fractured and is highly permeable [Winograd and Thordarson, 1975].

Numerous faults cut across Yucca Mountain in the model area [Scott and Bonk, 1984]. We treat the major faults as distinct hydrologic units. In general, faults at Yucca Mountain are conduits for flow along their strikes owing to fracturing and brecciation in the fault zones. Some faults may also be barriers to flow perpendicular to their strikes owing to offset stratigraphy or to fracture fillings. In the model area, we represented all of the faults as more permeable zones except for the inferred fault under the large hydraulic gradient, which is represented differently in each of the four conceptual models.

Hydrologic and physical properties

Hydrologic and physical properties (Table 1) were based primarily on laboratory and field data collected at Yucca Mountain. For porosity estimates, we collated data from a number of reports on core-sample measurements and well logs [Geldon, 1993; Nelson and Schimschal, 1993; Muller and Kibler, 1986; Waddell *et al.*, 1984; Lobmeyer *et al.*, 1983], and in some cases, we computed porosity from the difference between measurements of bulk density and grain density. The thermal conductivities chosen for the five hydrostratigraphic units are from Sass *et al.* [1988] who made 204 measurements of this parameter on core samples from boreholes in the Yucca Mountain area. Permeabilities (Table 1) were based on in-situ hydrologic tests conducted in bore holes [LeCain, 1996; Geldon, 1993; Montazer and Wilson, 1984; Waddell *et al.*, 1984]; however, the measured values cover a large range for each hydrologic unit and the number of measurements is statistically inadequate to establish reliable estimates of large-scale permeability, especially for the confining units. We therefore concentrated on choosing reasonable relative values for the different hydrologic units.

One of the main uncertainties in the hydrologic parameters used is the permeability

of fault zones because few direct field measurements are available. We estimated the permeability of the major exposed faults indirectly using the observed heat-flow anomalies along the Bow Ridge and Solitario Canyon faults [Fridrich *et al.*, 1994] and a solution from the one-dimensional heat conduction-convection theory [Bredehoeft and Papadopulos, 1967; Bodvarrson *et al.*, 1982]. We assumed that the heat flow low under northern Yucca Mountain (Figure 2) results from focused descent of relatively cool groundwater along some preferential pathways such as a fault. As the water migrates laterally at depth, it is heated by ambient geothermal flux. The warmed groundwater fluid then upwells along major exposed faults to the south, resulting in the observed relatively high heat flow under southern Yucca Mountain (Figures 2 and 3). We applied this conceptual model and derived the one-dimensional heat conduction-convection solution from Bredehoeft and Papadopulos [1965]:

$$J = K_t \frac{dT}{dz} = J_0 e^{D(z-z_0)} \tag{1}$$

where J is the heat flux, K_t is the thermal conductivity of the rock-fluid complex, T is temperature, z is the vertical coordinate, J_0 is the background geothermal heat flux at a datum z_0, parameter D is defined as $c_0 \rho_0 v/K_t$, c_o is the specific heat of the fluid, ρ_o is the density of the fluid, and v is the vertical groundwater velocity. Assuming a natural background temperature gradient of 30 degrees C/km, J_o = 63 mWm^{-2}, K_t=2.1 Watt/(meter °C), z_0=0, and z=100 m, for a velocity v of -3.5×10^{-9} m/s, the heat flux J will be 31 mWm^{-2}. This calculation suggests that a downward flow at the rate of 3.5×10^{-9} m/s will produce an apparent heat flow of 31 mWm^{-2}, which is lower than the background heat flow. Similarly, an upward flow velocity at 8×10^{-10} m/s will produce a heat flow high of 74 mWm^{-2}, similar to that observed in the southernmost part of the study area (Figure 2). Sass *et al.* [1988] estimated a vertical flow velocity of 3.2×10^{-9} m/s from the temperature profile in well USW G-1. From the estimated velocity and an assumed hydraulic gradient, one can estimate the hydraulic conductivity using Darcy's Law. If we assume a vertical hydraulic gradient of 0.01 in the recharge area, then the estimated vertical permeability is 3×10^{-14} m^2 in the fault. For a vertical hydraulic gradient of 0.001 in the discharge areas, the estimated permeability is 8×10^{-14} m^2 in the south.

Boundary conditions

The boundary conditions used in our models are in some cases artificial because insufficient data are available to determine the actual boundary conditions. At the upper boundary of our model, the ground surface, the pressure was set at the atmospheric value of 89,000 Pa, temperature was set at the annual mean temperature of 20 °C, and saturation was set at 20%. No local infiltration was assumed because existing data indicates it is minor relative to the lateral flow through the saturated-zone system. The base of our cross section is a no-flow boundary at which a constant heat flux of 53 mWm^{-2} [Sass *et al.*, 1988] was assigned; this is the average value over the study area (Figure 2). The sides of the model were set as constant head boundaries using water-table elevations that were

based on extrapolations from the observed water levels in wells USW G-2 and UE25p-1. On the sides, we assumed linear temperature profiles that were extrapolations from these same wells.

Quantitative Testing of Hypotheses

To test the hypotheses discussed earlier, we conducted numerical simulations, employing the parameters shown in Table 1 as a base case. The features distinguishing the three hypotheses are straightforward variations of permeability (Figure 4). Below, we compare the results of the different simulations, using the computed hydraulic gradients and water levels, as well as the calculated temperature profiles in the positions of the four wells along the model cross section.

Base model

To establish a starting point for testing different hypotheses, we set up a base model that contains the well-known hydrologic features of Yucca Mountain, but that omits all of the features that are hypothesized to cause the large hydraulic gradient. The hydrogeologic units that comprise the base model are discussed in descending order as follows (see Figure 3 and Table 1). The uppermost layer of the model is the Topopah Springs/Tiva Canyon formation, in which the water table is located. In the simulations, the position of the water table was computed using an exponential characteristic function (*i.e.*, van Genutchen model) describing unsaturated hydraulic permeability in this top layer. The underlying Calico Hills unit is subdivided into two layers because the lower part of this formation is more altered and therefore less permeable than the upper part. The next unit, the Crater Flat Group consists of the Prow Pass, Bullfrog, and Tram Tuffs and is the major Tertiary aquifer. This unit was given a southward-increasing permeability because hydrothermal alteration of these rocks increases to the north, as discussed above [Bish, 1989]. The underlying older tuff aquitard includes the Lithic Ridge Tuff, older tuffs, and an unnamed sedimentary section. This unit is a confining unit that separates the Tertiary tuff aquifer from the Paleozoic deep carbonate aquifer. The carbonate aquifer, at the bottom of the section, is divided into upper and lower layers. The Paleozoic carbonates were exposed at the surface prior to deposition of the Tertiary rocks. The top of the carbonates was therefore subjected to surficial weathering and fracturing, and is assigned greater permeability than the lower part. We assign all of the faults identified in the cross section with a moderate permeability (Table 1).

The results of the base model simulation are that: (1) Almost all of the groundwater flow is through the tuff aquifer under Yucca Mountain, because no mechanism was incorporated to introduce flow into the carbonate aquifer. (2) A zone of steeper hydraulic gradient is present in the calculated water-table configuration (Figure 5a) owing to the assumed southward increase in permeability of the Crater Flat tuff aquifer, but it is a poor fit to the observed water-table configuration. Specifically, the hydraulic gradients in the simulation are 0.07 in the north (between USW G-2 and USW G-1) and 0.02 in the south (between UE25-b#1 and UE25-p#1), as compared to the measured values of 0.15 and

0.001 in the same locations. (3) The downwelling that occurs under northern Yucca Mountain results in a reduced thermal gradient under the central part of the mountain, but the simulated thermal gradients are significantly different in detail from the profiles observed in the four Yucca Mountain wells in the cross section (not shown but similar to those of the spillway and dam models; Figure 6). Our conclusion from the base model simulation is that an additional feature(s) is needed in the simulation to create the observed water-table configuration and thermal structure of Yucca Mountain.

Spillway model

The spillway hypothesis assumes an abrupt southward increase in the magnitude and depth-extent of permeability in the Crater Flat tuff aquifer across the buried fault that underlies the large hydraulic gradient (Figure 4b). We tested this model by strongly reducing the permeability of the Crater Flat unit north of the buried fault relative to the base model, while all other parameters were kept the same. In the spillway-model simulation, the major flow is still through the tuff aquifer, as in the base model; however, the calculated water-table configuration is much closer to the observed pattern (Figure 5b). Specifically, the hydraulic gradients in the simulation are 0.16 in the north and 0.03 in the south, as compared to the measured values of 0.15 and 0.001.

The order-of-magnitude disagreement between the calculated and observed hydraulic gradient in the south can be explained by the fact that, to the east and west of the model cross section, the Topopah Spring Tuff becomes a significant part of the Tertiary aquifer system on the downgradient side of the large hydraulic gradient [Fridrich *et al.*, 1994]; hence, the average transmissivity under southern Yucca Mountain is greater than that in the model cross section. We thus consider that the large hydraulic gradient is successfully reproduced by the spillway model.

The simulated thermal regime for the spillway model is similar to that of the base model. When the observed temperature profiles in the four wells of the cross section are compared with those computed in the spillway model simulation (Figure 6), they agree well in the upper part of the section, but diverge significantly at depth. The simulated temperatures are too high within the carbonate aquifer (in well UE25-p#1) and in the lower, confining-unit part of the volcanic section.

Drain model

The drain model postulates that the large hydraulic gradient is caused by focussed downwelling of the majority of the flow passing through the tuffs under northern Yucca Mountain into the carbonate aquifer under central and southern Yucca Mountain (Figure 4a). We tested this scenario by increasing the permeability of the buried fault under the large hydraulic gradient by one order of magnitude, while all other parameters were kept the same as in the base run. In our simulation, approximately half of the flow through the tuffs is captured by the carbonate aquifer at the large hydraulic gradient. The computed hydraulic gradient is 0.08 in the north and 0.015 in the south (Figure 5c), as compared to the measured values of 0.15 and 0.001. As with the spillway model, we consider this to

be an adequate fit to the water-table configuration, given the limitations of a two-dimensional model.

The drain model predicts the presence of a thermal low on the downgradient side of the the large hydraulic that extends several kilometers to the south. The fit between the calculated and observed thermal profiles in the four wells on the cross section is reasonably good in the shallow parts of the section (Figure 6c), but diverges significantly at depth. Specifically, the calculated temperatures are too low in the deeper part of section at the bottom of the large hydraulic gradient (in the location of well USW G-1) and too high in the carbonate aquifer in the location of well UE25-p#1 (Figure 6c).

Dam model

In the dam model, the large hydraulic gradient is produced by inserting a narrow, high-angle planar zone of low permeability in the position of the buried fault under northern Yucca Mountain (Figure 4c). The flow regime is similar to that of the spillway and base models. The computed hydraulic gradients are 0.07 in the north and 0.03 in the south (Figure 5d), as compared to the measured values of 0.15 and 0.001. As with the previous models, this is considered an adequate fit for our purposes. The thermal regime and the calculated thermal profiles in the positions of the four wells in the model cross section are almost identical to those calculated in the spillway model (Figure 8).

Discussion and Conclusions

All three of the hypotheses we considered for the large hydraulic gradient - dam, drain, and spillway - provide an adequate simulation of the observed water-table configuration under Yucca Mountain, given the limitations of a two-dimensional model. It is probable that exact fits could be achieved by adjusting the permeability structures in the models; however, our purpose was testing of hypotheses rather than achieving exact fits.

All three models also provide an adequate simulation of the shallow thermal regime under Yucca Mountain. None of the models, however, provide an adequate simulation of the deep thermal regime, and the drain model alone can be eliminated on that basis. The simulations of the drain model show that, if the thermal low observed at northern Yucca Mountain was caused by downwelling from the tuff aquifer into the carbonate aquifer along the buried fault between drill holes USW G-1 and USW G-2, then the thermal gradient at the base of the large gradient (in the vicinity of USW G-1) should be extremely low, much lower than was observed (Figure 6). We consider the drain model to be disproven by this result because of the very large difference between the observed and simulated value, and because the physical process that underlies the simulated value is inherent to the concept of the drain model.

The deep thermal regimes simulated for the dam and spillway models do not match the observed regime either; however, this does not present the same problem because these two models include no prediction about groundwater flow processes in the carbonate aquifer. For the dam and spillway models, the misfit can be resolved by invoking an external process -- cool underflow through the carbonate aquifer. That invokation can be

justified because the heat flow anomaly under Yucca Mountain is part of the regional-scale Eureka Low, and because the Eureka Low as a whole is considered to be caused by cool underflow through the carbonate aquifer, as discussed above.

The model results demonstrate that downwelling within the tuff aquifer at the large hydraulic gradient, and related processes, can explain the short-wavelength details of the thermal anomaly under Yucca Mountain, and the dam and spillway models appear equally acceptable in this regard. The spatial coincidence of the lowest point in the heat-flow anomaly with the large hydraulic gradient (Figure 2) is strong circumstantial evidence for a causative relation between these two features. The next lowest part of the thermal anomaly is a trough aligned along the major fault block that comprises Yucca Mountain, with relative thermal highs along the major faults on either side (in Solitario Canyon and on the east side of Midway Valley; Figure 2). The geometry of the anomaly is consistent with the concept that, across the large hydraulic gradient, the potentiometric head in the tuff aquifer drops below that in the underlying confined carbonate aquifer, so that some upward leakage occurs along the major faults that cut the intervening confining unit to the south [Fridrich *et al.*, 1994]. The gradual increase in the heat flow to the south reflects the gradual heating of the water in tuff aquifer, southward of the point of downwelling, owing to both ambient geothermal heating and to inmixture of warmer water upwelling from the carbonate aquifer. Isotopic discontinuities in the groundwater provide independent evidence for the upwelling of water from the carbonate aquifer into the tuff aquifer under southern Yucca Mountain [Stuckless *et al.*, 1991].

The fact that the short-wavelength details of the thermal anomaly under Yucca Mountain are well explained by the flow regime in the tuff aquifer does not prove that the entire heat-flow low is caused by flow processes in the tuff aquifer. In all of our simulations, we assumed that the heat flow at the base of the models was 53 mWm-2, a value that was derived by averaging the heat flow observed in the unsaturated zone over the study area (the area with heat flow contours in Figure 2). The 53 mWm-2 value thus represents a reasonable estimate of the heat flow at the water table, and probably is a close estimate of the heat flow at the base of the Tertiary volcanic section. It may, however, be a poor reflection of the heat flow at the base of the hydrologic system, which is typically about 100 mWm-2 in most of the Great Basin. The lower heat flows observed in the near surface in most of the area of the Eureka Low, relative to the rest of the Great Basin, have been explained as being caused by removal of heat by groundwater flow within the carbonate aquifer. The abundance of hot springs and other evidence of high advective heat flows in the discharge areas in the Death Valley groundwater system (Winograd and Thordarson, 1975), as well as in other parts of the Eureka Low, suggests that a significant amount of heat is redistributed by the hydrologic system and that the heat flows observed in wells throughout much of the rest of the system (outside of the discharge areas) are depressed relative to the ambient heat flow at the base of the system.

The inverted slope in the thermal profile observed in the deeper part of drill hole UE-25p#1 (Figure 6) indicates either (1) that significant vertical flow was occurring in the bore hole during measurement of the profile or (2) that there is strong lateral flow within the carbonate aquifer in the vicinity of this bore hole. Either way, this profile is not representative of the thermal regime in the carbonate aquifer under Yucca Mountain as a

whole. Moreover, the very low bottom-hole temperature in UE-25p#1 is almost certainly a local anomaly and is probably associated with channelized flow through a fracture system that was encountered in the deeper part of this hole. Although local in nature, the magnitude of this anomaly nonetheless supports the interpretation that flow in the carbonate aquifer under Yucca Mountain significantly modifies the ambient heat-flow.

The dominant process controlling the long-wavelength part of the heat-flow anomaly at Yucca Mountain is probably flow within the deep carbonate aquifer and is evidently unrelated to the large hydraulic gradient. This conclusion is appealing for two reasons. First, the heat flow low at Yucca Mountain is a very small part of a regional feature, the Eureka Low (Figure 2, inset map). A regional process - groundwater flow through the carbonate aquifer - thus appears to provide a better explanation than one that is based on a local hydrologic feature. Second, hydrochemical data from Yucca Mountain indicate that the water in the carbonate aquifer has about ten times the chlorine abundance of the water in the tuff aquifer [La Camera and Westerburg, 1994]. These data do not, by themselves, disprove the drain model; however, they can be reconciled with it only through special pleading.

The dam and spillway models both appear acceptable as physical-process explanations for the large hydraulic gradient, given existing hydrologic and heat-flow data. However, these two models yield strongly contrasting predictions about the pattern of vertical hydraulic gradients in the immediate vicinity of the large hydraulic gradient (Figure 5, A and D). It appears likely that the details of the potentiometric regimes calculated in these simulations could change significantly with the addition of the third dimension, and with changes in boundary-condition assumptions that currently are poorly constrained. Nonetheless, the very large difference in the simulated potentiometric patterns for these two models suggest that a well-designed drilling and hydrologic testing program that targets the immediate area of the large hydraulic gradient would yield data that could provide definitive answers about the cause of this feature.

References

Bath, G.D. and C.E. Jahren, 1984, Interpretations of magnetic anomalies at a potential repository site located in the Yucca Mountain area, Nevada Test Site, U.S. Geological Survey Open-File Report, 84-120, 40pp.

Bish, D. L., 1989, Evaluation of past and future alterations in tuff at Yucca Mountain, Nevada, based on clay mineralogy of drill cores USW G-1, G-2, and G-3: Los Alamos National Laboratories, Los Alamos, NM, Report LA-10667-MS, 42 p.

Bodvarrson, G., S.M. Benson, and P.A. Witherspoon, 1982, Theory of the development of geothermal systems charged by vertical faults, Jour. Geophys. Res., 87(B11), 9317-9328.

Boynton, G.R. and J.L. Vargo, 1963, Aeromagnetic map of the Topopah Spring Quadrangle and part of the Bare Mountain Quadrangle, Nye County, Nevada, U.S. Geological Survey Geophysical map GP-440, 1 sheet, 1:62 500.

Bredehoeft, J.D. and S.S. Papadopulos, 1965, Rates of vertical groundwater movement estimated from the earth's thermal profile, Water Resources Research, 1(2), 325-328.

Craig, R.W. and J.H. Robison, 1984, Geohydrology of the rocks penetrated by well UE-25p1, Yucca Mountain area, Nye County, Nevada, U.S. Geological Survey Water-Resources Investigation Report, 84-4248, 57pp.

Czarnecki, J.B. and R.K. Waldell, 1984, Finite-Element Simulation of Ground-Water Flow in the Vicinity of Yucca Mountain, Nevada-California, U.S. Geological Survey Water-Resources Investigation Report, 84-4349, 38pp.

Czarnecki, J., 1994, Is there perched water under Yucca Mountain in borehole USW G-2? EOS, American Geophysical Union Fall Meeting, abs., 249-250.

Czarnecki, J.B., P.H. Nelson, G.M. O'Brien, J. Sass, B. Thapa, Y. Matsumoto, and O. Murakami, 1995, Testing in borehole USW G-2 at Yucca Mountain: the saga continues, EOS, American Geophysical Union Fall Meeting, abs., 190.

Ervin, E.M., R.R. Luckey, and D.J. Burkhardt, 1994, Revised Potentiometric-Surface Map, Yucca Mountain and Vicinity, Nevada, U.S. Geological Survey Water-Resources Investigations Report 93-4000, 17pp.

Fridrich, C.J., W.W. Dudley, Jr., and J.S. Stuckless, 1994, Hydrogeologic analysis of the saturated-zone ground-water system, under Yucca Mountain, Nevada, Jour. Hydrology, 154, 133-168.

Geldon, A.L., 1993, Preliminary hydrogeologic assessment of boreholes UE-25c #1, UE-25c#2, UE-25c#3, Yucca Mountain, Nye County, Nevada, U.S. Geological Survey Water-Resources Investigation Report, 92-4016.

Haws, S.J., 1990, The Distribution of Vertical Groundwater Flow in the Saturated Zone of the Yucca Mountain Area: a Cross-Sectional Finite Element Model, Master Thesis, University of Las Vegas, 120pp.

Hinds, J., C. Fridrich, and S. Ge, 1997, Perched water dynamics at Yucca Mountain, Nevada: a numerical approach, in *Hydrology Days*, Proceedings of the Seventeenth Annual American Geophysical Union, 127-140.

Jasek, N.A., 1991, Simulated Effects of Changes in the Infiltration Rate and the Hydraulic

Conductivity Structure on the Location and Configuration of the Water Table at Yucca Mountain, Nevada, Master Thesis, Texas A&M University, 70pp.

LeCain, G.D., 1996, Air-injection testing in vertical boreholes in welded and nonwelded tuff, Yucca Mountain, Nevada, U.S. Geological Survey Water-Resources Investigation Report 96-4262.

La Camera, R. J., and Westerburg, C. L., 1994, Selected ground-water data for Yucca Mountain region, southern Nevada and eastern California, through December, 1992: U. S. Geological Survey Open-File Report 94-54, 161 pp.

Lachenbruch, A.H. and J.H. Sass, 1977. Heat flow in the United States and the thermal regime of the crust, in The Earth's Crust, edited by J.G. Heacock, Geophysical Monograph 20, American Geophysical Union, Washington, D.C., 626-675.

Lobmeyer, D.H., M.S.Whitfield, Jr, R.G. Lahoud, and L. Bruckheimer, 1983, Geohydrologic data for test well UE-25b-1, Nevada Test Site, Nye County, Nevada, U.S. Geological Survey Open-File Report, 83-855, 52pp.

Marshall, B.D., Z.E. Peterman, and J.S. Stuckless, 1993, Strontium isotopic evidence for a higher water table at Yucca Mountain: Proceedings of the Fourth International Conference on High-Level Radioactive Waste Management, American Nuclear Society, 2, 1948-1952.

Montazer, P. and W. E. Wilson, 1984, Conceptual hydrologic model of flow in the unsaturated zone, Yucca Mountain, Nevada, U.S. Geological Survey Water-Resources Investigation Report, 84-4345.

Muller, D.C. and J.E. Kibler, 1986, Preliminary analysis of geophysical logs from the WT series of drill holes, Yucca Mountain, Nye County, Nevada, U.S. Geological Survey Open-File Report, 86-46, 30 pp.

National Research Council (NRC), 1992, Ground Water at Yucca Mountain, How High Can it Rise, National Academy Press, Washington D.C., 231pp.

Nelson P.H. and U. Schimschal, 1993, Assessment of geophysical logs from borehole USW G-2, Yucca Mountain, Nevada, U.S. Geological Survey Open-File Report, 92-572.

Pruess, K., 1991, TOUGH2 - A General-Purpose Numerical Simulator for Multiphase Fluid and Heat Flow, Lawrence Berkeley Laboratory, CA, 102pp.

Robison, J.H., 1984, Ground-water Level Data and Preliminary Potentiometric Surface Maps, Yucca Mountain and Vicinity, Nye County, Nevada, U.S. Geological Survey Water-Resources Investigation Report 84-4197, 8pp.

Rousseau, J.P., E.M. Kwicklis, and D.C. Gillies, 1996, Hydrogeology of the unsaturated zone, north ramp area of the exploratory studies facility, Yucca Mountain, Nevada, U.S. Geological Survey Water-Resources Investigation Report, 272pp.

Sass, J.H., W.W. Dudley, Jr., A.H. Lachenbruch, 1995, Chapter 8: Regional thermal setting, in Oliver, H.W., Ponce, D.A., and Hunter, W.C., Major Results of Geophysical Investigations at Yucca Mountain and Vicinity, Southern Nevada: U.S. Geological Survey Open-File Report 95-74, 199-218.

Sass, J.H., A.H. Lachenbruch, W.W. Dudley, Jr., S.S. Priest, and R.J. Munroe, 1988, Temperature, thermal conductivity, and heat flow near Yucca Mountain, Nevada: some tectonic and hydrologic implications, U.S. Geological Survey Open-File

Report 87-649, 118pp.
Sass, J.H., A.H. Lachenbruch, R.J. Munroe, G.W. Greene, and T.H. Moses, Jr., 1971, Heat flow in the western United States, Jour. Geophys. Res., 76, 6376-6413.
Scott, R.B. and J. Bonk, 1989, Preliminary geologic map of Yucca Mountain with geologic sections, Nye County, Nevada, U.S. Geophysical Survey Open-File Report 84-494, 3 sheets, 1:12000.
Sinton, P.O., 1989, Three-Dimensional, Steady-State, Finite-Difference Model of the Groundwater Flow System in the Death Valley Groundwater Basin, Nevada-California, Master thesis, Colorado School of Mines, 145pp.
Stuckless, J. S., Whelan, J. F., and Steinkampf, W. C., 1991, Isotopic discontinuities in ground water beneath Yucca Mountain, Nevada: High-Level Radioactive Waste Management, 2nd Int. Symp., Las Vegas, NV, 28 April - 1 May, 1991, v. 2, p. 1410-1415, American Nuclear Society, La Grange, IL.
Waddell, R.K., 1982, Two-dimensional, steady-state model of ground-water flow, Nevada Test Site and vicinity, Nevada-California, U.S. Geological Survey Water-Resources Investigation, 82-4085, 72pp.
Waddell, R.K., J.H. Robinson, and R.K. Blankennagel, 1984, Hydrology of Yucca Mountain and vicinity, Nevada-California - Investigation results through mid-1983, U.S. Geological Survey Water-Resources Investigation Report 84-4267, 72pp.
Winograd, I.J. and W. Thordarson, 1975, Hydrogeologic and hydrochemical framework, south-central Great Basin, Nevada-California, with special reference to the Nevada test Site, U.S. Geological Survey Professional Paper 712-C, 126pp.

Figure 1. Location map of Yucca Mountain (YM) in the southern Great Basin in relation to the boundaries of the southwest Nevada volcanic field and the Death valley ground-water system.

Figure 2. Map of the Yucca Mountain area with the water-table configuration, the pattern of heat flow in the unsaturated zone, and the locations of deep bore holes as black dots (modified from Robison [1984], Ervine *et al.*, [1994] and Sass, et al. [1988; 1995]. Bedrock area is shown by light shading. Yucca Mountain is the dendriform bedrock area occupying the west side of the figure. Line A-A' is the line of section shown in Figure 3.

Figure 3. North-northwest -- south-southeast cross section across Yucca Mountain based on subsurface geology and gravity data; taken from Fridrich *et al.* [1994]. Since this figure was drafted, the Prow Pass, Bullfrog, and Tram Members of the Crater Flat Tuff have been formally renamed as the Prow Pass, Bullfrog, and Tram Tuffs of the Crater Flat Group (Sawyer and others, 1994). The Eleana Argillite (Formation), projected into this cross section from the Calico Hills based on an inteterpretation of aeromagnetic data (Bath and Jahren, 1984), has since been reclassified as Chainman Shale (J. C. Cole, USGS, oral comm., 1997).

Figure 4. Schematic illustrations of the three hypotheses for the cause of the large hydraulic gradient: (a) drain model, (b) spillway model, (c) dam model.

Figure 5. Simulated potentiometric regimes for: (A) the base model, (B) the spillway model, (C) the drain model, and (D) the dam model.

Figure 6. Comparison of the simulated (lines) and observed (boxes) thermal profiles for the (A) spillway model, (B) dam model, and (C) drain model, in the four wells that lie along the cross section used.

Table 1. Summary of hydrologic and physical properties used in the model

Hydrostratigraphic Unit	Permeability m^2	Density kg/m^3	Porosity	Thermal Conductivity W/m °C
Tiva Canyon/Topopah Spring	10^{-15}	2600	0.2	1.87
Calico Hills upper	10^{-15}	2400	0.35	1.22
lower	10^{-16}	2400	0.35	1.22
Crater Flat Tuff Aquifer				
north & central	10^{-15}	2600	0.20	1.59
south	10^{-14}	2600	0.20	1.59
Tuff Aquitard	10^{-16}	2700	0.2	1.96
Carbonate Aquifer upper	10^{-13}	2700	0.20	4.90
lower	10^{-14}	2700	0.20	4.90
Buried fault	10^{-14}	2700	0.2	1.96
Faults in the south	10^{-14}	2700	0.2	1.96

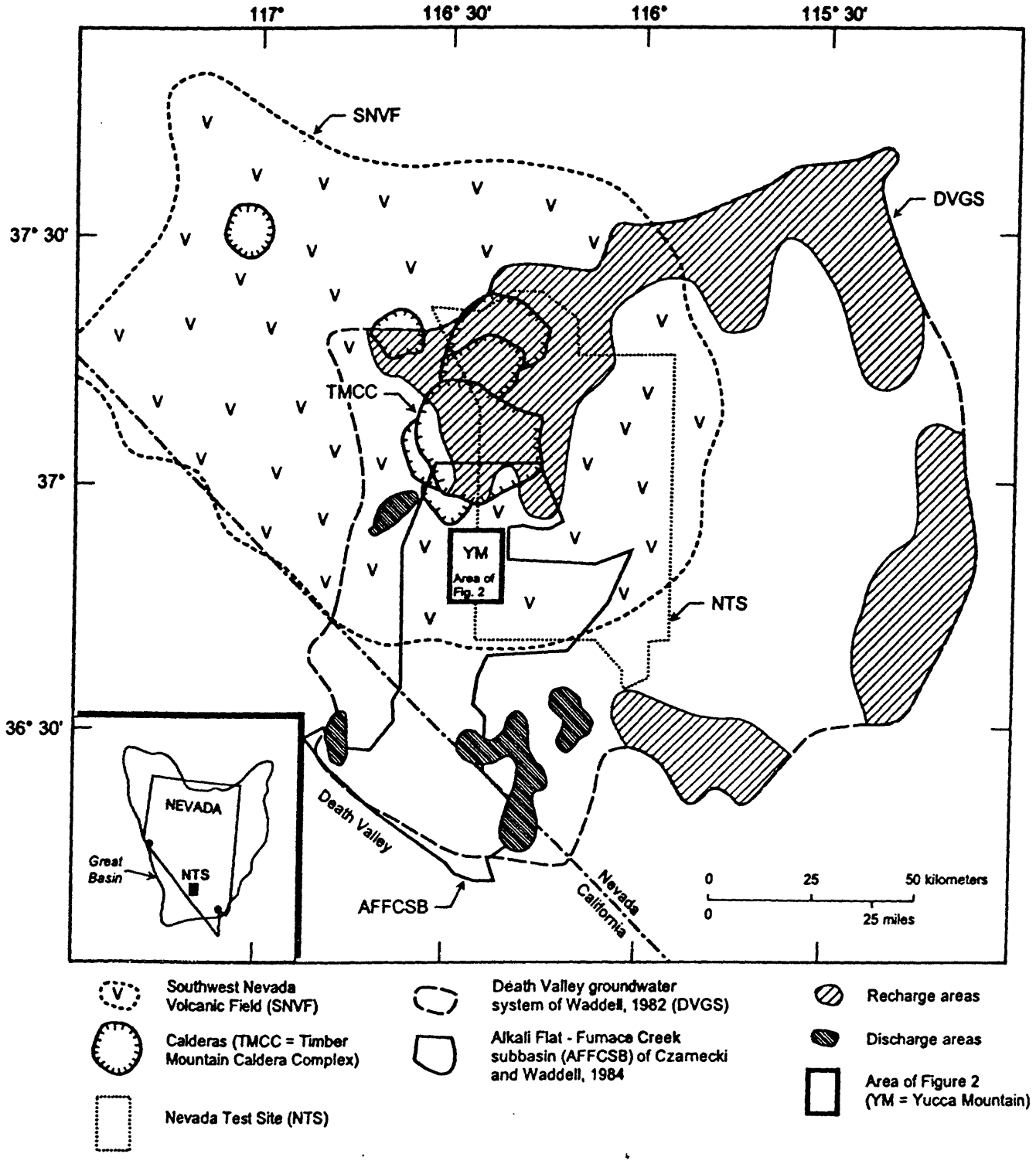
117°
116° 30'
116°
115° 30'
37° 30'
37°
36° 30'
SNVF
DVGS
TMCC
YM
Area of Fig. 2
NTS
NEVADA
Great Basin
NTS
Death Valley
AFFCSB
Nevada
California
0
25
50 kilometers
0
25 miles
Southwest Nevada Volcanic Field (SNVF)
Calderas (TMCC = Timber Mountain Caldera Complex)
Nevada Test Site (NTS)
Death Valley groundwater system of Waddell, 1982 (DVGS)
Alkali Flat - Furnace Creek subbasin (AFFCSB) of Czamecki and Waddell, 1984
Recharge areas
Discharge areas
Area of Figure 2 (YM = Yucca Mountain)

FIGURE 1

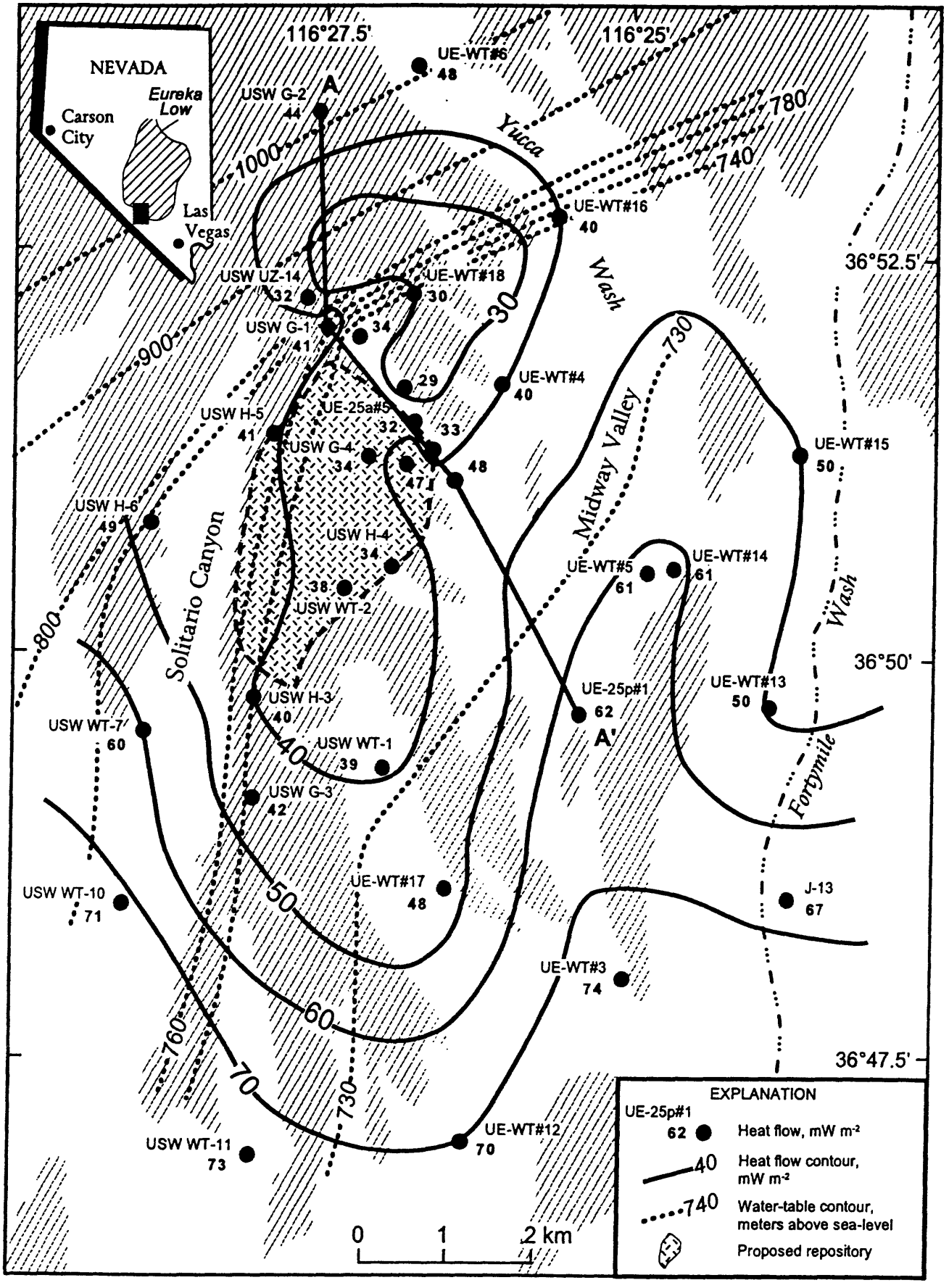
NEVADA
Eureka Low
Carson City
Las Vegas
116°27.5'
116°25'
36°52.5'
36°50'
36°47.5'
A
A'
USW G-2 44
UE-WT#6 48
UE-WT#16 40
USW UZ-14 32
UE-WT#18 30
USW G-1 41
34
29
UE-WT#4 40
USW H-5 41
UE-25a#5 32
33
USW G-4 34
47
48
USW H-6 49
USW H-4 34
38
USW WT-2
UE-WT#5 61
UE-WT#14 61
UE-WT#15 50
UE-25p#1 62
UE-WT#13 50
USW H-3 40
USW WT-7 60
USW WT-1 39
USW G-3 42
UE-WT#17 48
J-13 67
USW WT-10 71
UE-WT#3 74
UE-WT#12 70
USW WT-11 73
1000
900
800
780
740
730
760
Yucca Wash
Midway Valley
Solitario Canyon
Forty mile Wash
30
40
50
60
70
0 1 2 km
EXPLANATION
UE-25p#1
62
Heat flow, mW m-2
40
Heat flow contour, mW m-2
740
Water-table contour, meters above sea-level
Proposed repository

FIGURE 2

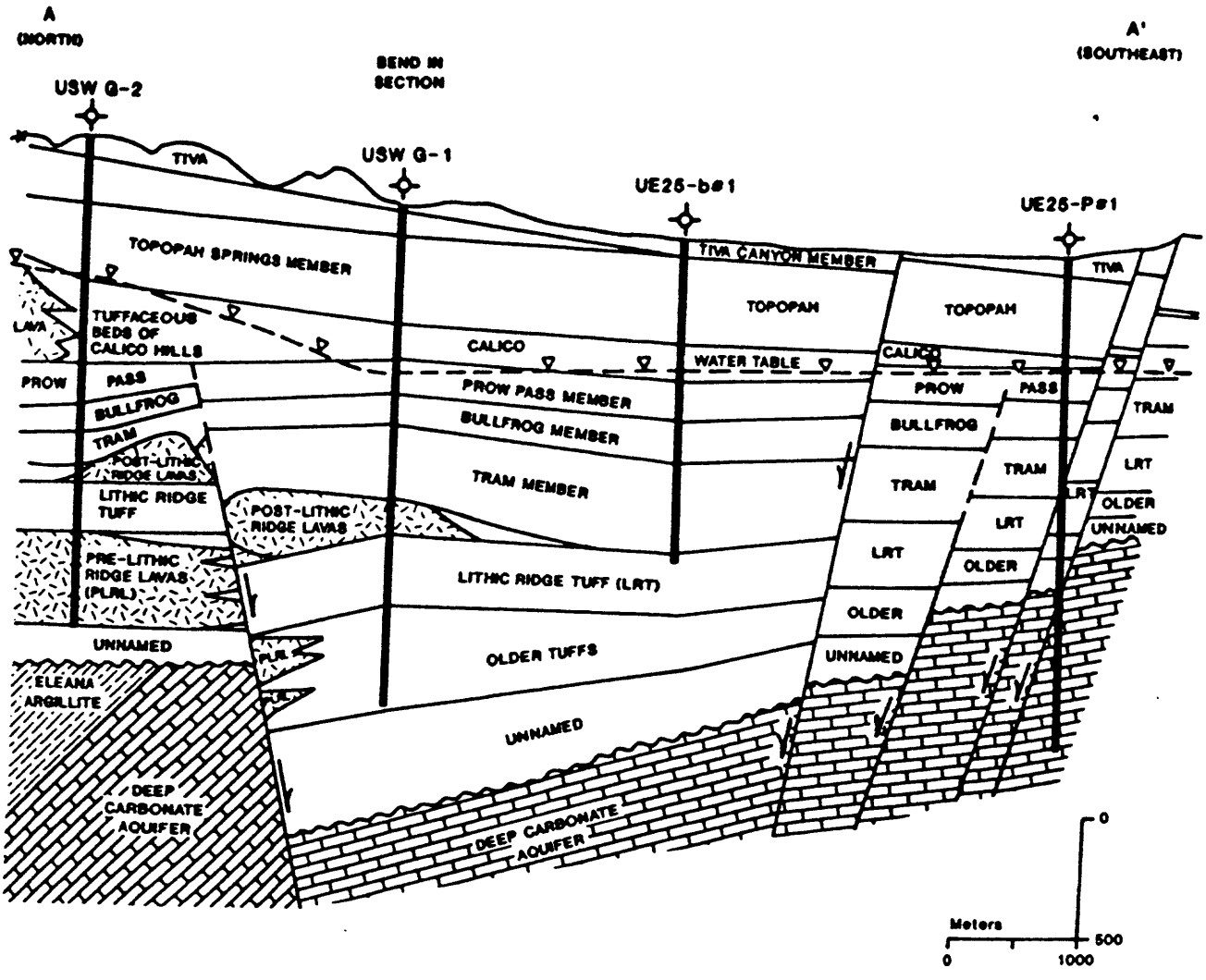
A
(NORTH)
A'
(SOUTHEAST)
USW G-2
BEND IN SECTION
USW G-1
UE25-b#1
UE25-P#1
TIVA
TOPOPAH SPRINGS MEMBER
TIVA CANYON MEMBER
TOPOPAH
TUFFACEOUS BEDS OF CALICO HILLS
CALICO
WATER TABLE
PROW PASS MEMBER
PROW
PASS
BULLFROG
BULLFROG MEMBER
TRAM
TRAM MEMBER
POST-LITHIC RIDGE LAVAS
LITHIC RIDGE TUFF
LRT
OLDER
UNNAMED
PRE-LITHIC RIDGE LAVAS (PLRL)
LITHIC RIDGE TUFF (LRT)
OLDER TUFFS
ELEANA ARGILLITE
DEEP CARBONATE AQUIFER
Meters
0
500
1000

FIGURE 3

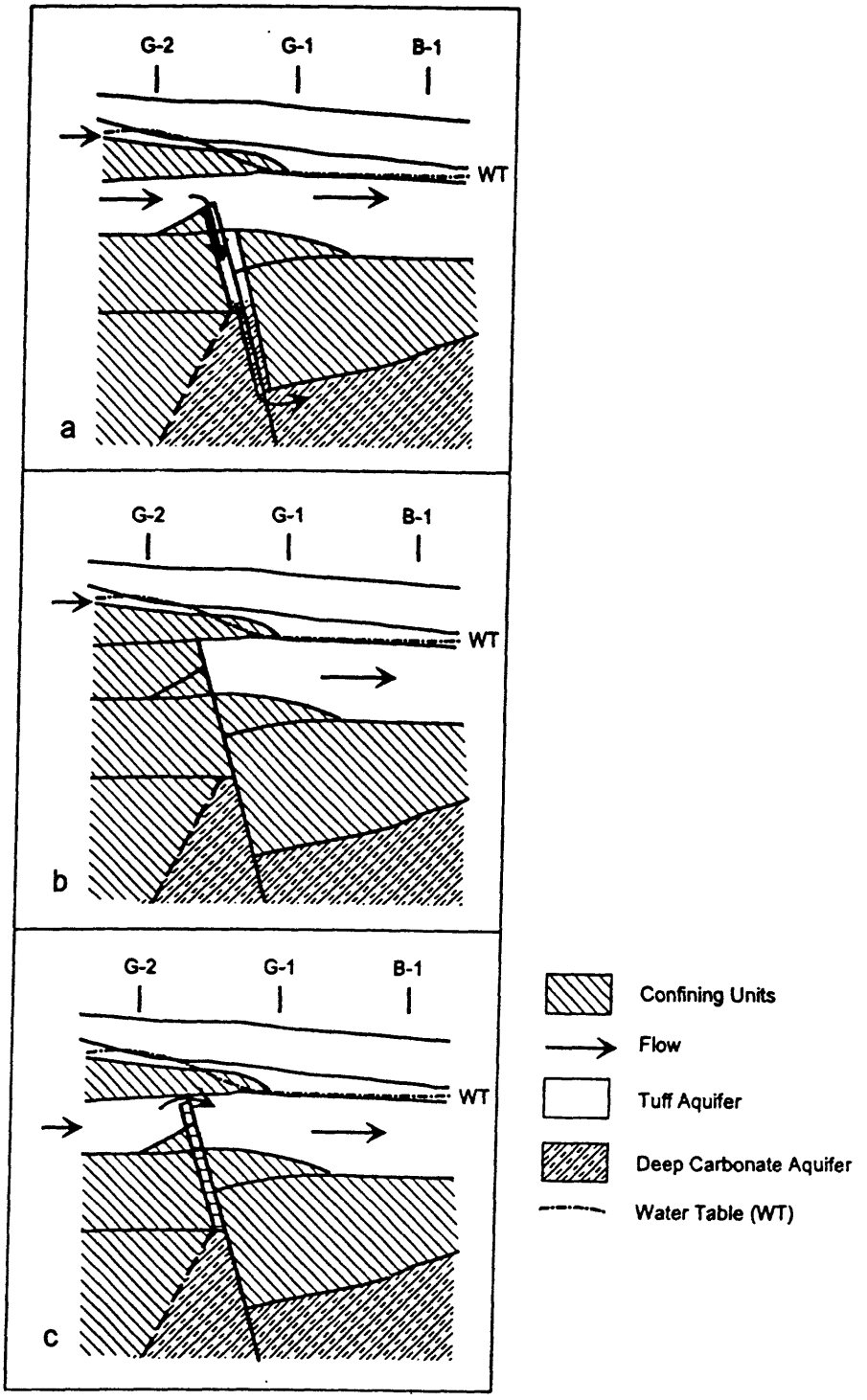
G-2
G-1
B-1
WT
a
G-2
G-1
B-1
WT
b
G-2
G-1
B-1
WT
c
Confining Units
Flow
Tuff Aquifer
Deep Carbonate Aquifer
Water Table (WT)

FIGURE 4

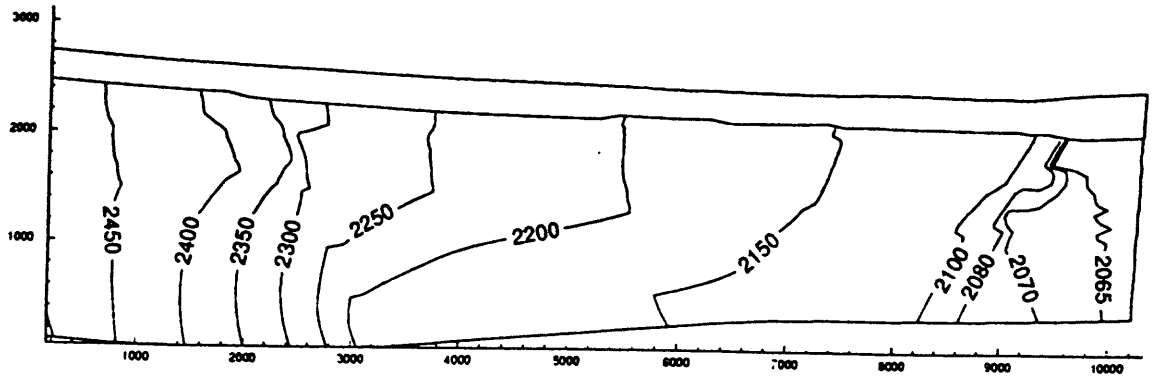

A

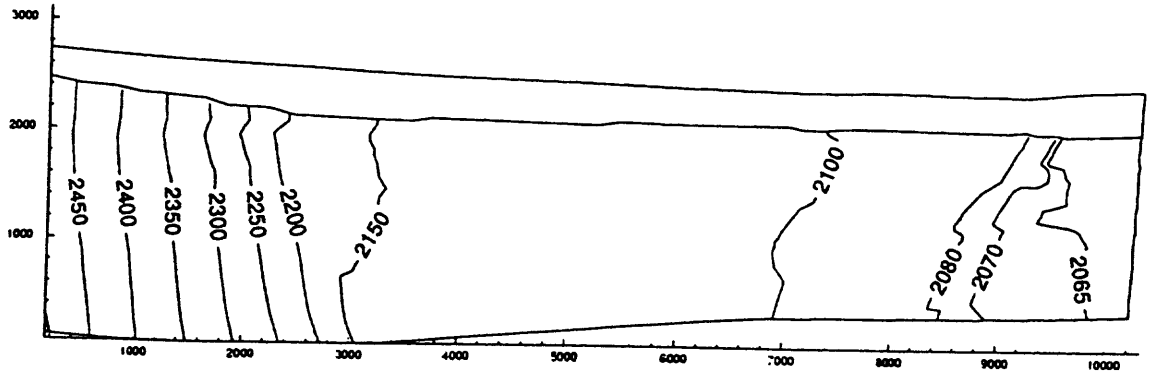

B

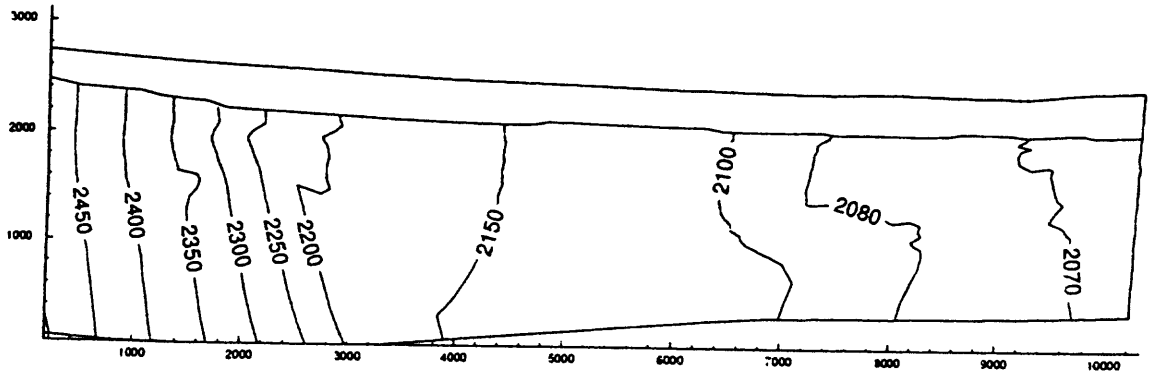

C

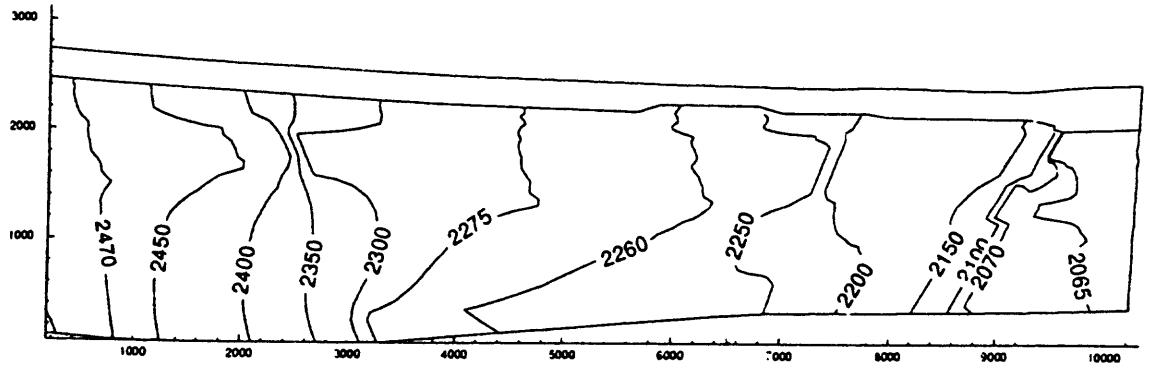

D

FIGURE 5

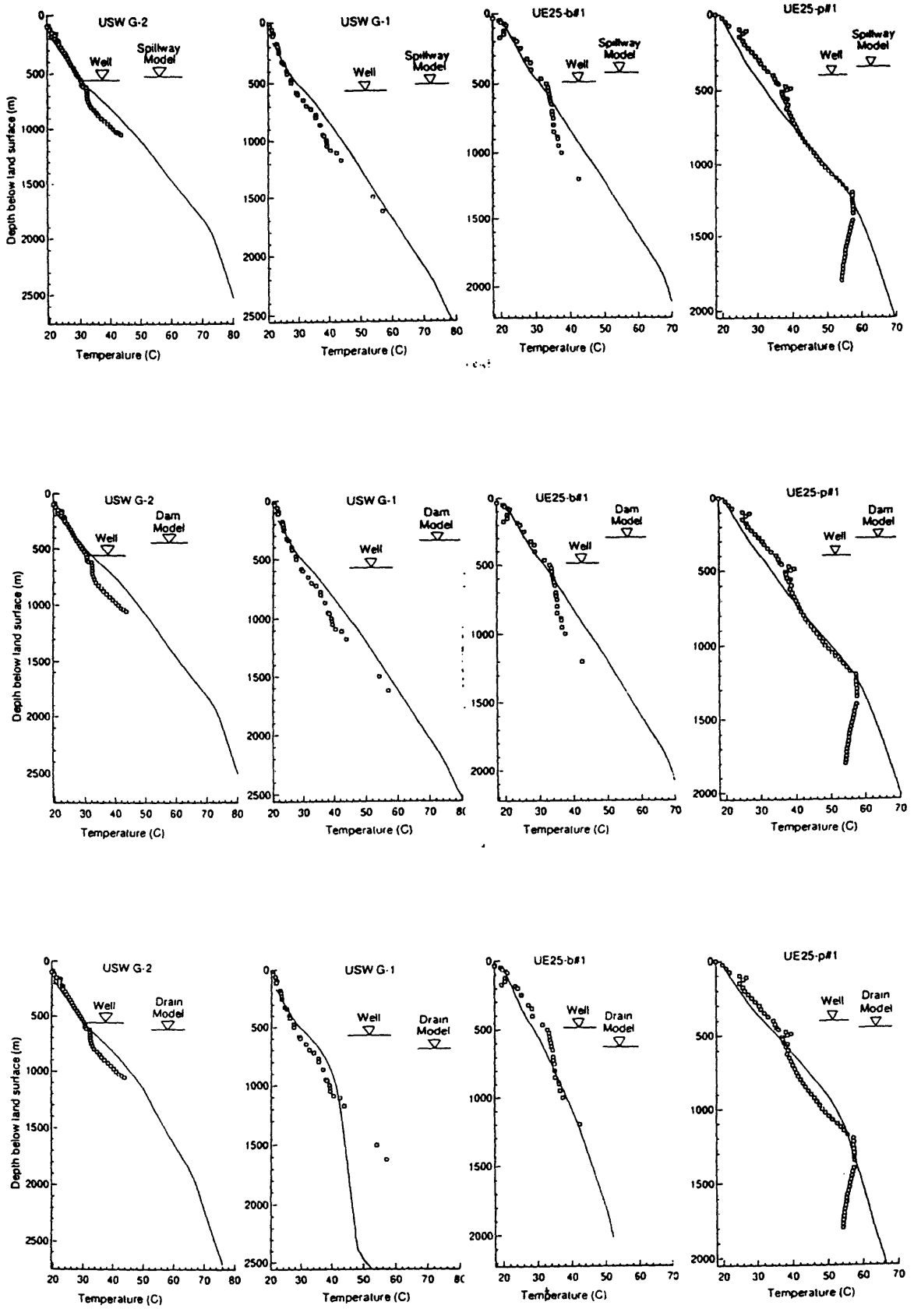
A
B
C
USW G-2
USW G-1
UE25-b#1
UE25-p#1
Well
Spillway Model
Dam Model
Drain Model
Depth below land surface (m)
Temperature (C)

FIGURE 6